View metadata, citation and similar papers at core.ac.uk
brought to you by CORE
provided by Universidade do Minho: RepositoriUM

Plasma Process. Polym. 2009, 6, S760–S766

The Role of Modulated IR Radiometry Measurements in the Characterization of Zr-O-N Thin Films

F. Macedo[1], P. Carvalho[2], L. Cunha[1], F. Vaz[2], Jurgen Gibkes[3],Bruno K. Bein[3], Josef Pelzl[3]

[1]Centro de Fìsica, Universidade do Minho, Campus de Gualtar, 4710-057 Braga, Portugal
[2]Centro de Fìsica, Universidade do Minho, Campus de Azurém, 4800-058 Guimarães, Portugal
[3]Exp.Phys.III, Solid State Spectroscopy, Ruhr-University Bochum, D-44780 Bochum, Germany

Abstract

This work is devoted to the investigation of relevant thermal transport parameters of multifunctional ZrOxNy thin films, prepared in strict controlled conditions. Composition and structural characterizations revealed the existence of two different types of films, with a structural change from fcc ZrN to Zr3N4-type. Modulated IR radiometry was used to screen out these internal changes, and also to prove its importance and application viability within complicate systems such as thin films. The thermal diffusion time of the coatings and the ratio of the thermal effusivities coating-to-substrate were directly determined. Empirical correlations between processing conditions, the films' composition and structure, and thermal transport properties were found.

Introduction

In today's modern technology, the increasing demand for low cost production and reduced material resources is inducing a change in what was most traditional in thin film R&D—the search for new material combinations and new element additions to well-known systems.[1–4] This was clearly the route that was followed in the early eighties and nineties, when, for example, Al,[5] Si[6,7] and several other elements (alone or together) were added to TiN to improve its oxidation resistance and mechanical/tribological performance.[1–7]

This type of approach, based on specific actions that consist in the development of new and more complex systems (which could reach more than five elements), has brought an increasing number and detailed methods of analysis that needed further developments in order to proceed with the thin film system towards its industrial implementation. Anyway, the complexity of such systems is so high that the up-scaling requires a huge amount of efforts that may not compensate the improvement in a particular application. In more recent years, the materials R&D starts to become more interested to explore the potential of already available and well-known material systems, whose combination of properties already suggests further application fields.

Within this alternative approach, one can include the case of the PVD produced metal oxynitride thin films, MeO_xN_y (Me = early transition metal), which—due to their multifuncionality—are gaining increasing importance in today's technical coatings. Their relevance arises from the fact that the presence of oxygen allows the tailoring of film properties between those of metallic nitrides, MeN_y, and those of the correspondent insulating oxides, MeO_x, and thus, by tuning the oxide/nitride ratio, it is possible to tune the crystallographic order between oxide and nitride and hence the electronic structure and consequently the physical properties of the materials. The decorative field has already profited from this wide 'property-tailoring

F. Macedo, L. Cunha
Department of Physics, University of Minho, Campus de Gualtar, 4710-057 Braga, Portugal
E-mail: fmacedo@fisica.uminho.pt
P. Carvalho, F. Vaz
Department of Physics, University of Minho, Campus de Azurém, 4800-058 Guimarães, Portugal
J. Gibkes, B. K. Bein, J. Pelzl
Exp.Phys.III, Solid State Spectroscopy, Ruhr-University Bochum, D-44780 Bochum, Germany

possibilities' of the oxynitrides, allowing to prepare different intrinsic coloured surfaces.[8,9]

Taking this into account, the main purpose of this work consists of the preparation of single layered zirconium oxynitrides, ZrO_xN_y thin films, with a clear focus on their thermal properties to allow future applications beyond those of decoration,[9] where heated surfaces, time-dependent heat transition problems and thermal mechanisms may play an important role.

Another objective of this work is to explore the possibilities of modulated IR radiometry and to show its ability to study layer systems, since controlled changes in the heating modulation frequency can reveal the thermal depth profile of the samples and thus the different thermal properties of each layer. The correlation of the thermal properties with the changes in composition and crystalline structure will be the main focus of this work.

To perform this study a set of ZrO_xN_y samples were prepared in straight controlled conditions, varying only in the gas mixture flow ($N_2 + O_2$ — 19:1 ratio) during the films production. In section II, details of the production and characterization of the thin films are presented, as well as a brief description of the setup used for modulated IR radiometry. In section III the main equations used for the quantitative determination of the thermal parameters determination are explained. In section IV, the experimental results are presented: the composition and structural analysis, the thermal transport properties and the correlations between composition, structural properties and thermal properties with the coatings' process conditions. The main conclusions are given in section V.

Film Deposition and Applied Measurement Methods

For the present work, the ZrO_xN_y films (with intrinsic colours only) were deposited on high speed steel (AISI M2) substrates by reactive DC magnetron sputtering, using a laboratory-sized deposition system (home-made), composed of two vertically opposed rectangular magnetrons (unbalanced of type 2), in a closed field configuration. The films were prepared with the substrate holder positioned at 70 mm from the target in all runs, using a DC current density of $100\,A \cdot m^{-2}$ on the Zr target ($200 \times 100\,mm^2$ — 99.6 at.-% purity). A gas atmosphere composed of argon (working gas) and nitrogen + oxygen reactive mixture (95% N_2 + 5% O_2) was used for the depositions. The argon flow was kept constant at 60 sccm in all depositions, while the mixed reactive gas flow varied from 4 to 17.5 sccm (corresponding to partial pressure variations between 3.2×10^{-2} and 1.6×10^{-1} Pa). The working pressure changed only slightly between ≈0.4 and 0.5 Pa. The effective pumping speed was adjusted to $356\,L\,s^{-1}$. The substrates were grounded and no external heating was applied.

The atomic composition of the as-deposited samples was measured by Rutherford Backscattering Spectroscopy (RBS) using a 2 MeV He^+ beam as well as 1.4 and 2 MeV proton beams, to increase the accuracy in the oxygen signals. CALOTEST® was used to measure the thickness of the samples. The structure and phase distribution of the coatings were accessed by X-ray diffraction (XRD), using a conventional Philips PW 1710 diffractometer and operating with Cu $K\alpha$ radiation in a Bragg–Brentano configuration.

For the depth-resolved measurements of the films' thermal transport properties, thermal waves have been excited using an Argon ion laser beam, intensity-modulated by means of an acousto-optical modulator, as pump beam. The used range of heating modulation frequencies extended from 1 to 100 kHz. This allowed to resolve surface layer in-homogeneities, thin films and coatings in the range from below 1 micron to several microns. The photothermal signal is measured using an IR optical system consisting of two BaF_2 IR lenses of 50 mm radius, a Ge IR filter and a nitrogen-cooled HgCdTe IR detector. To filter the valid information from the detector response, a two-phase lock-in amplifier was used. A more detailed description of the setup used for modulated IR radiometry can be found in ref.[10]

Quantitative Interpretation of Modulated IR Radiometry Applied to Coatings

Details of modulated IR radiometry, the measurement technique and quantitative interpretation in the case of thin films, can be found in ref.[11,12] The data directly obtained by modulated IR radiometry are the in-phase and out-of phase thermal wave signals, filtered with the help of the Lock-in amplifier at the modulation frequency of excitation from the IR radiation emitted by the coating.[13] For the quantitative interpretation, the signals measured for coating-substrate systems have to be calibrated with the help of reference data measured for a homogeneous opaque body of smooth surface.[14] Considering a two-layer model, with the first layer representing the coating (c) and the second layer the backing (b) respectively the substrate, and applying the *Extremum method*,[15] it is possible to determine the coatings' thermal diffusion time τ_c and the ratio of the thermal effusivities (e_c/e_b) coating-to-substrate from the relative extrema $\{f_{extr}, \Phi_{n\ extr}\}$ of the measured inverse calibrated phase lag signals:

$$\tau_c = \frac{d_c^2}{\alpha_c} = \frac{1}{4\pi f_{extr}} \left\{ 0.5 \arccos[(\tan\ \Phi_{n\ extr})^2] \right\}^2 \qquad (1)$$

$$\left(\frac{e_c}{e_b}\right) = \frac{\sqrt{(k\rho c)_c}}{\sqrt{(k\rho c)_b}} = \frac{(1+R_{cb})}{(1-R_{cb})} \quad (2)$$

with the thermal reflection coefficient:

$$R_{cb} = \mp\sqrt{\frac{1-\tan\{0.5\arccos[(\tan\ \Phi_{n\,extr})^2]\}}{1+\tan\{0.5\arccos[(\tan\ \Phi_{n\,extr})^2]\}}} \exp\left\{0.5\arccos[(\tan\ \Phi_{n\,extr})^2]\right\} \quad (3)$$

determined directly from the measured relative extrema of the inverse calibrated phase lag signals. The negative sign in Equation (3) is used for relative minima, i.e., for coatings, the thermal effusivity $\sqrt{(k\rho c)_c}$ of which is smaller than the effusivity of the substrate and the positive sign is used for coatings, the effusivity of which is larger than the effusivity of the substrate. Once the coating thickness d_c is known from independent measurements (Section II), the thermal diffusivity of the coating $\alpha_c = d_c^2/\tau_c$ can immediately be calculated. In addition, if the thermal effusivity of the substrate e_b is known, the heat capacity $(\rho \cdot c)_c = (e_c/\alpha_c^{1/2})$ and the thermal conductivity $k_c = (e_c \cdot \alpha_c^{1/2})$ of the coatings can also be determined.[16]

To get information on the coatings' thermal parameters, the intermediate range of modulation frequencies, $25 < (f/\mathrm{Hz})^{1/2} < 125$ is here considered, neglecting the deviations from the two-layer model at very high modulation frequencies, which may be due to very thin surface layers of the coating with differing thermo-optical properties.[17] Similarly, the deviations from the two-layer model at very low modulation frequencies are neglected, which are related to the coating-to-substrate heat transition and to the heat propagation, mainly inside the substrate.[17,18]

Results and Discussion

Composition

Figure 1 shows the elemental concentration and the variations of atomic ratios for the ZrO_xN_y coatings analysed in the frame of this work.

The first point worth to be mentioned about these results is the relative smoothened variation in the elemental concentrations, with the increase in the gas flow, Figure 1a). This is an important feature for theses films due to the well-known high affinity of oxygen towards metals (about one hundred times more reactive than nitrogen[19,20]). The fact that the gas mixture is composed of an excess of nitrogen (N_2:O_2 ratio of 19:1) and the depositions are carried out with a relatively high pumping speed ($356\,L \cdot s^{-1}$), a gradual transition between the metallic and compound state of the target is obtained, inducing a smooth composition variation, as well as the non-existence of an early oxide phase as it will be shown later on in this paper. This allows to obtain a large variation of different ZrO_xN_y coatings which behave completely different from the typical oxide-like type. Despite apparent small variations, Figure 1b shows that the films prepared with reactive gas flows below 8 sccm exhibit the largest changes in the atomic ratios. Particularly noticeable is the increase in the C_N/C_{Zr} ratio approaching the value 1.1 (close stoichiometric), for the coating deposited with that particular gas flow (8 sccm). Above that gas flow value, this ratio seems to become approximately constant around the value of 1.1. Moreover, the ratio C_O/C_{Zr} is relatively low (around 0.1) up to the sample prepared with a gas flow of 8 sccm, and thus, there seems to be some favourable conditions to form some kind of close stoichiometric ZrN compounds (with some possible oxygen inclusions[9]).

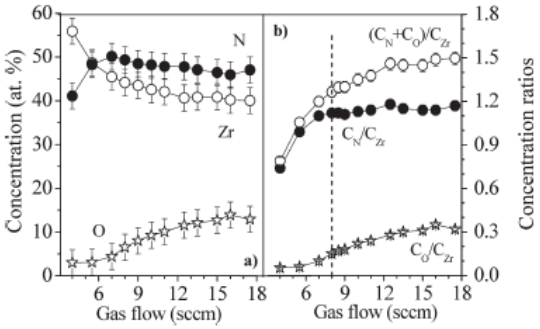

Figure 1. Variation of the: (a) atomic concentration of the elements as a function of the reactive gas mixture flow; and (b) non-metals over the zirconium atomic ratios, C_O/C_{Zr}, C_N/C_{Zr} and $(C_N + C_O)/C_{Zr}$ as a function of the reactive gas mixture flow.

The films prepared with reactive gas flows ≥8 sccm show a slow but systematic increase in oxygen: — The atomic ratio C_O/C_{Zr} increases about three times to ≈0.3 (Figure 1b) and it is expected that it plays an important role for the samples prepared in this region of gas flows. Although the ratio C_N/C_{Zr} remains approximately constant in the samples prepared with these high gas flows (≥8 sccm), the increase in the oxygen content results in a relatively high ratio of non-metallic to metallic elements, $[(C_N + C_O)/C_{Zr}]$, which increases also smoothly from about 1.1 (for the 8 sccm sample) to about 1.5 (for the 16 sccm sample). The almost no variation of nitrogen content and the reactively high over-stoichiometric condition of the films prepared with gas flows above 8 sccm (if one takes into account the values of the ratio $[(C_N + C_O)/C_{Zr}]$, might be an indication for the possibility to form overstoichiometric nitride compounds.

Structure

In order to analyse the effects of variations in chemical composition on the films' crystalline structure and to

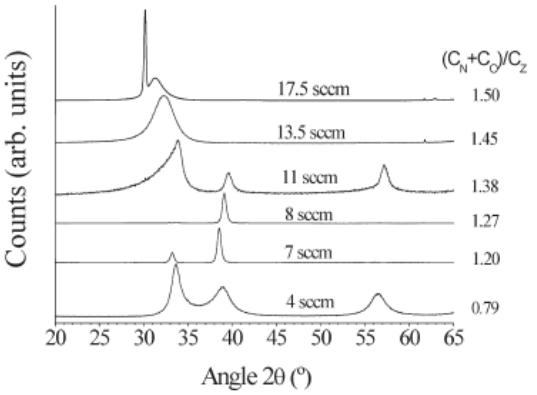

Figure 2. XRD patterns for a selection of the analysed ZrO_xN_y films.

confirm whether the films are in fact all similar in structural terms or, in contrast, there are different crystalline structures and thus also a variation in the films' properties (the claimed multifunctionality within the film system), a detailed structural characterization has been carried out. Figure 2 shows XRD patterns for some of the coatings prepared in the different composition zones previously discussed.

From this figure it is possible to conclude that, despite rather small changes in composition, there are different groups of coatings with respect to the particular structural arrangement. There seem to be slightly different limits for the different zones when the effects of composition and structure were compared directly. Moreover, and following the smooth variations in composition, the diffractograms of Figure 2 show that the transition from one crystalline-type structure to the other involves always a significant number of samples.

In terms of specific structural features, Figure 2 shows that the samples deposited with reactive gas flows up to 11 sccm, which presented a non-metal to zirconium ratio $(C_N + C_O)/C_{Zr}$, varying from ≈0.8 to ≈1.4, crystallized in a B1-NaCl crystal structure, typical for ZrN, with a progressive change of the preferential growth from ⟨111⟩ to ⟨200⟩, with the increase in the reactive gas flow. Beyond the particular crystallinity, these results enabled to clear out some doubts about the different types of samples present in this study, which the composition plots could hardly reveal.

Regarding the X-ray diffractograms (Figure 2) for films prepared with reactive gas flows between 11 [$(C_N + C_O)/C_{Zr} = 1.38$] and 17.5 sccm [$(C_N + C_O)/C_{Zr} = 1.50$], the results suggest the development of a crystalline structure that does not seem to match anymore with that of fcc ZrN. Moreover, the results reveal a smooth transition from the previous fcc NaCl-type structure (sample deposited with a reactive gas flow up to 11 sccm [$(C_N + C_O)/C_{Zr}$ up to 1.38] towards a new one. The reduced number of diffraction peaks associated with a significant peak broadening does not allow fully accurate indexing of this structure. Anyway, the broadening of the peak at $2\theta \approx 32.2°$, which corresponds to a shift from the (111) reference ZrN of about 2 °C could result from a small grain size and/or some reduction of the crystalline volume fraction of the coating, or even from a superposition of several peaks predicted in this region of the structure, suggesting the formation of an overstoichiometric nitride phase close to that of Zr_3N_4.[9,21,22]

Despite the similarities of the structural arrangement for the films deposited with gas flows between 11 sccm [$(C_N + C_O)/C_{Zr} = 1.38$] and 17.5 sccm [$(C_N + C_O)/C_{Zr} = 1.50$], Figure 2 shows that — for the films deposited with reactive gas flows higher than 15 sccm [$(C_N + C_O)/C_{Zr} > 1.45$] — there is already the beginning of another structure. In a previous work,[9] this new phase had been analysed in detail and indexed to a cubic structure similar to that of γ-Zr_2ON_2 (ICDD card no. 48-1635).[23,24]

These results demonstrated that the changes in chemical composition are inducing a change in the crystalline structure of the films, and consequently, changes are expected in the films' thermal properties.

Thermal

In Table 1, the measured thermal data are presented, namely the phase values and the modulation frequencies at the relative extrema, as well as the deduced coatings' thermal parameters.

As discussed in section II and shown by Equation (2) and (3), the values (e_c/e_b) are directly determined from the measured quantities $\Phi_{n\ extr}$. It is noteworthy that a directly measurable thermal quantity, namely the values of the phase extrema $\Phi_{n\ extr}$ correlate with the deposition parameters, namely with the gas flow and thus also with composition and structure.

In Figure 3, the main thermal coating parameters obtained by modulated IR radiometry are presented as functions of the atomic concentration ratio $(C_N + C_O)/C_{Zr}$. In this figure it is interesting to see that both the thermal diffusivity and the effusivity ratio show a rather clear, general correlation with the atomic concentration ratio $(C_N + C_O)/C_{Zr}$. In addition one can see, that the samples which revealed the ZrN-type growth with atomic concentration ratio $(C_N + C_O)/C_{Zr}$ below 1.38, have got higher values for both the thermal diffusivity, $\alpha_c > 8 \cdot 10^{-7}\ m^2 \cdot s^{-1}$, and the effusivity ratios $(e_c/e_b) > 0.32$, indicating thus also the existence of direct correlations between structure and thermal properties.

A closer look at Figure 2 shows that the sample prepared with a gas flow of 11 sccm (revealing an atomic ratio [$(C_N + C_O)/C_{Zr}$ of 1.38] is still presenting the ZrN-type crystallites, together with a large tail in the region

Table 1. Measured phase extrema (f_{extr}, $\Phi_{n\ extr}$) and directly deduced thermal coating parameters (τ_c, e_c/e_b).

Sample code	Conc. ratio	O_2 flow	$\Phi_{n\ extr}$	$(f_{extr})^{1/2}$	τ_c	e_c/e_b	d_c	a_c	$(\rho c)_c$	k_c
	$(C_N + C_O)/C_{Zr}$	sccm	deg	$Hz^{1/2}$	μs		μm	$m^2\ s^{-1}$	$J\ m^{-3}\ K^{-1}$	$W\ m^{-1}\ K^{-1}$
P17	1.29	8.5	−16.3	64.0	1.07E-05	0.39	3.666	1.3E-06	2.96E+06	3.7
P14	1.30	9	−16.3	64.0	1.07E-05	0.39	3.337	1.0E-06	3.25E+06	3.4
P05	1.35	10	−18.2	64.0	1.04E-05	0.35	3.522	1.2E-06	2.68E+06	3.2
P06	1.38	11	−19.5	64.0	1.01E-05	0.32	2.983	8.8E-07	2.86E+06	2.5
P09	1.46	12.5	−21.7	57.0	1.22E-05	0.27	2.888	6.8E-07	2.77E+06	1.9
P10	1.45	13.5	−20.9	64.0	9.86E-06	0.29	2.618	7.0E-07	2.92E+06	2.0
P11	1.45	15	−22.2	51.0	1.51E-05	0.26	3.159	6.6E-07	2.71E+06	1.8
P12	1.49	16	−21.2	57.0	1.24E-05	0.28	2.71	5.9E-07	3.09E+06	1.8
P13	1.50	17.5	−20.1	57.0	1.26E-05	0.31	2.585	5.3E-07	3.53E+06	1.9

The thermal diffusivity α_c has been calculated based on additional independent measurements of the coating's thickness d_c. The volume heat capacity $(\rho c)_c$ and the thermal conductivity k_c have been calculated considering the ratio of the effusivities (e_c/e_b) and literature data (Bohler Steel technical datasheet) for the thermal effusivity $e_b = \sqrt{(k\rho c)_b}$ of the high speed steel (AISI M2) substrate.

$30° < 2\theta < 35°$, a sign of the appearance of the Zr_3N_4-type phase. On the other hand, for the samples prepared in the Zr_3N_4 'dominant' zone $(C_N + C_O)/C_{Zr}$ above 1.38, Figure 2 shows that the samples are now clearly dominated by this type of crystalline growth and the thermal parameters show now more pronounced reductions. Furthermore, this change in structural characteristics may also be seen in the last sample (the one prepared with a gas flow of 17.5 sccm — $[(C_N + C_O)/C_{Zr} = 1.50]$. This sample showed in the XRD diffractograms (Figure 2), the beginning of the appearance of a 'new' type of crystallites: those of a γ-Zr_2ON_2-type phase. Similarly to what has been observed within the transition from ZrN to Zr_3N_4-type samples (Figure 2). This sample reveals a comparatively higher value of the effusive ratio, together with a smaller value of the thermal diffusivity, although its atomic ratio is very similar to that of the previous sample $(C_N + C_O)/C_{Zr} \approx 1.49$, prepared with a gas flow of 16 sccm. Again, these results show a clear influence of the structural effects (induced by those of composition changes) on the thermal behaviour, which go beyond the particular chemical composition of the particular samples.

In Figure 4 one may clearly distinguish two main different sets of samples: at the very surface, the coatings with $(C_N + C_O)/C_{Zr}$ values in the range from 1.45 to 1.50 (films from the second zone, with an orthorhombic Zr_3N_4-type structure) considerably exceed the Zero-line $\Phi_n = 0$, and thus exhibit a three-layer structure with a very thin

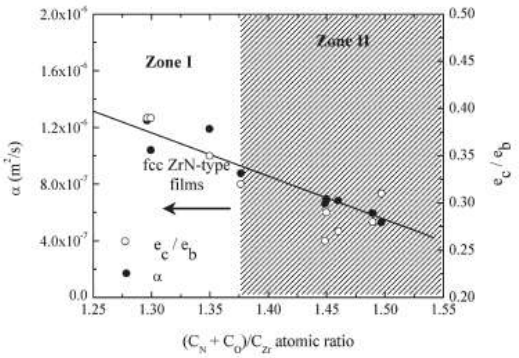

Figure 3. Thermal diffusivity of the coatings and ratio of the thermal effusivities coating-to-substrate for the analysed ZrO_xN_y films.

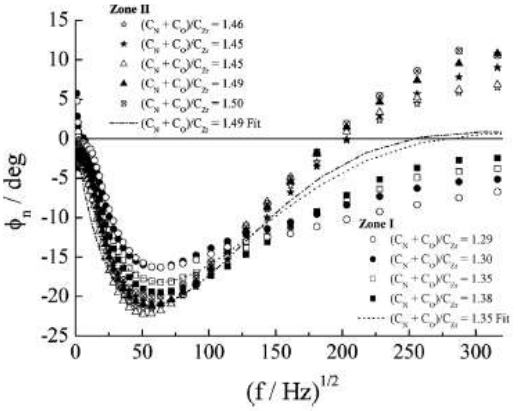

Figure 4. Inverse calibrated IR phases obtained for the ZrO_xN_y films, compared to two-layer approximations for samples with concentration ratios of 1.35 (dots) and 1.49 (dashed-dotted line).

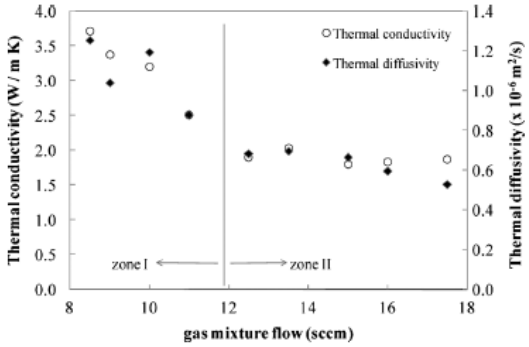

Figure 5. Thermal diffusivity and conductivity as a function of the gas mixture flow during processing.

layer on top of the coating of higher thermal transport properties, while the two-layer approximations (dotted and dashed dotted lines) follow the Zero-line. In contrast to that behaviour, the samples with atomic ratios $(C_N + C_O)/C_{Zr}$ varying between 1.29 and 1.38 (films from the first zone, which developed a ZrN-type structure) do not cross or follow the Zero-line, exhibiting a three-layer structure with a thin layer on top of the coating of comparatively lower thermal transport properties. These differences follow closely the changes in composition (Figure 1) and thus also changes in the crystalline structure.

Figure 5 presents the thermal diffusivity and thermal conductivity as a function of the gas mixture flow during processing. An interesting feature associated with the behaviour shown in Figure 5 is the clear decrease in the thermal diffusivity and conductivity values with increasing gas mixture flow. Comparing the behaviour of the thermal diffusivity with that shown in Figure 3 (α_c vs. composition), one can see a more pronounced trend, pointing towards a clear dependence of the coating's thermal properties on the process conditions. For a gas mixture flow above 12 sccm (zone II), the values of the referred thermal properties remain nearly constant, reflecting thus the transition to a more insulating structure corresponding to Zr_3N_4, in contrast to the ZrN-type structure in Zone I.

Conclusion

The analysed ZrO_xN_y films were prepared by DC reactive magnetron sputtering; using a reactive gas mixture composed of 95% N_2 + 5% O_2. The composition variations were obtained by increasing the gas flow, taking profit of the higher reactivity of oxygen leading to increased oxygen content. The characterization of the variations in composition (especially the atomic ratios) allowed to conclude that there are two different types of coatings.

Structural characterization revealed a strong dependence of the film texture on the oxygen content; exhibiting a change from fcc-type films of low oxygen content for low gas flows to a structure similar to that of Zr_3N_4 with oxygen inclusions at higher gas flows. These compositional and structural changes showed clear correlations with the effective thermal transport properties, e.g., the thermal diffusivity and conductivity, determined by depth-resolved measurements based on modulated IR radiometry. Modulated IR radiometry combined with the inverse solution for the two-layer thermal wave problem revealed to be a powerful tool to determine the thermal transport properties of coating-substrate systems.

At higher heating modulation frequencies, corresponding to shorter thermal penetration depths, deviations from the two-layer model have been found, corresponding to coatings with thin surface layers on top of the coatings with differing thermal transport properties. Thin surface layers of both comparatively higher and lower thermal transport properties have been found, and these variations of the coatings' surface properties also have been found to correlate with the coatings' composition and crystalline structure.

Received: September 16, 2008; Accepted: May 24, 2009; DOI: 10.1002/ppap.200931802

Keywords: coatings; dc magnetron sputtering; modulated IR radiometry; thermal properties; Zr–O–N

[1] O. Knotek, M. Böhmer, T. Leyendecker, F. Jungblut, *Mater. Sci. Eng.* **1988**, *105–106*, 481.
[2] H. A. Jehn, F. Thiergarten, E. Ebersbach, D. Fabian, *Surf. Coat. Technol.* **1991**, *50*, 45.
[3] O. Knotek, F. Löffler, A. Schrey, B. Bosserhoff, *Surf. Coat. Technol.* **1993**, *61*, 133.
[4] S. Heck, T. Emmerich, I. Munder, J. Steinebrunner, *Surf. Coat. Technol.* **1996**, *86–87*, 467.
[5] H. A. Jehn, S. Hofmann, W.-D. Münz, *Thin Solid Films* **1987**, *153*, 45.
[6] F. Vaz, L. Rebouta, P. Goudeau, J. Pacaud, H. Garem, J. P. Rivière, A. Cavaleiro, E. Alves, *Surf. Coat. Technol.* **2000**, *133–134*, 307.
[7] S. Veprek, S. Reiprich, *Thin Solid Films* **1995**, *268*, 64.
[8] F. Vaz, P. Cerqueira, L. Rebouta, S. M. C. Nascimento, E. Alves, Ph. Goudeau, J. P. Rivière, K. Pischow, J. de Rijk, *Thin Solid Films* **2004**, *447–448*, 449.
[9] P. Carvalho, J. M. Chappé, L. Cunha, S. Lanceros-Méndez, P. Alpuim, F. Vaz, E. Alves, C. Rousselot, J. P. Espinós, A. R. González-Elipe, *J. Appl. Phys.* **2008**, *103*, 104907.
[10] F. Macedo, A. Gören, A. C. Fernandes, F. Vaz, J. Gibkes, K. H. Junge, J. L. Nzodoum-Fotsing, B. K. Bein, *Plasma Processes Polym.* **2007**, *4*(S1), 857.
[11] F. Macedo, F. Vaz, A. C. Fernandes, J. L. Nzodoum-Fotsing, J. Gibkes, J. Pelzl, B. K. Bein, *Plasma Proc. Polym.* **2009**, DOI: ppap.200931503

[12] F. Macedo, F. Vaz, A. C. Fernandes, L. Rebouta, S. Carvalho, K. H. Junge, B. K. Bein, *Plasma Processes Polym.* **2007**, *4*(S1), 190.
[13] C. A. Bennett, R. R. Patty, *Appl. Opt.* **1982**, *21*, 49.
[14] DIN EN 15042-2:2006, "*Thickness measurement of coatings and characterization of surfaces with surface waves*".
[15] J. L. Nzodoum Fotsing, J. Gibkes, J. Pelzl, B. K. Bein, *J. Appl. Phys.* **2005**, *98*, 063522.
[16] F. Macedo, A. Goren, F. Vaz, J. L. Nzodoum Fotsing, J. Gibkes, B. K. Bein, *Vacuum* **2008**, *82*, 1461.
[17] F. Macedo, F. Vaz, L. Rebouta, P. Carvalho, A. Haj-Daoud, K. H. Junge, J. Pelzl, B. K. Bein, *Vacuum* **2008**, *82*, 1457.
[18] J. L. Nzodoum Fotsing, B. K. Bein, J. Pelzl, *Superlattices Microstruct.* **2004**, *35*, 419.
[19] N. Martin, R. Sanjines, J. Takadoum, F. Lévy, *Surf. Coat. Technol.* **2001**, *142–144*, 615.
[20] S. H. Mohamed, O. Kappertz, J. M. Ngaruiya, T. Niemeier, R. Drese, Wakkad, M. Wuttig, *Phys. Stat. Sol. (A)* **2004**, *201*, 90.
[21] D. I. Bazhanov, A. A. Knizhnik, A. A. Safonov, A. A. Bagatur'yants, M. W. Stoker, A. A. Korkin, *J. Appl. Phys.* **2005**, *97*, 044108.
[22] L. Pichon, T. Girardeau, A. Straboni, F. Lignou, P. Guérin, J. Perrière, *Appl. Surf. Sci.* **1999**, *150*, 115.
[23] M. Lerch, *J. Mater. Sci. Lett.* **1998**, *17*, 441.
[24] I. Milosev, H. Strehblow, M. Gaberscek, B. Navinsek, *Surf. Interface Anal.* **1996**, *24*, 448.